

# Successive Cancellation Ordered Search Decoding of Modified $G_N$ -Coset Codes

Peihong Yuan, *Student Member, IEEE*, and Mustafa Cemil Coşkun, *Student Member, IEEE*

**Abstract**—A tree search algorithm called successive cancellation ordered search (SCOS) is proposed for  $G_N$ -coset codes that implements maximum-likelihood (ML) decoding by using an adaptive search schedule. The average complexity is close to that of successive cancellation (SC) decoding for practical frame error rates (FERs) when applied to polar and Reed-Muller (RM) codes with block lengths up to 128. By modifying the algorithm to limit the worst-case complexity, one obtains near-ML performance for longer RM codes and their subcodes. Unlike other bit-flip decoders, no outer code is needed to terminate decoding so SCOS also applies to modified  $G_N$ -coset codes with dynamic frozen bits. SCOS decoding is further extended by forcing it to look for candidates satisfying a threshold, thereby outperforming basic SCOS decoding under complexity constraints. Simulations with a (128,64) polarization-adjusted convolutional code show gains in overall and undetected FER as compared to polar codes concatenated with an outer cyclic redundancy check code under SC list decoding at high signal-to-noise ratio over binary-input additive white Gaussian noise channels.

**Index terms**— Complexity-adaptive maximum-likelihood decoding, error detection, polar codes, Reed-Muller codes.

## I. INTRODUCTION

$G_N$ -coset codes are a class of block codes [2] that include polar codes [2], [3] and Reed-Muller (RM) codes [4], [5]. Polar codes achieve capacity over binary-input discrete memoryless channels (B-DMCs) under low-complexity successive cancellation (SC) decoding [2] and RM codes achieve capacity over binary erasure channels (BECs) under maximum-likelihood (ML) decoding [6].<sup>1</sup> However, their performance under SC decoding [3] is not competitive for short- to moderate-lengths, e.g., from 128 to 1024 bits [8].<sup>2</sup> Significant research effort has been put into approaching ML performance by modifying the SC decoding schedule and/or improving the distance properties [10]–[43].

The idea of *dynamic* frozen bits lets one represent any linear block code as a *modified*  $G_N$ -coset code [23]. This concept unifies the concatenated polar code approach, e.g., with a high-rate outer cyclic redundancy check (CRC) code, to improve the

distance spectrum of polar codes so that they can be decoded with low to moderate complexity [22].

This paper proposes *successive cancellation ordered search* (SCOS) as a ML decoder for modified  $G_N$ -coset codes. The decoding complexity adapts to the channel noise and an extension of SCOS limits the worst-case complexity while still permitting near-ML decoding. The decoder can be used for  $G_N$ -coset codes or CRC-concatenated  $G_N$ -coset codes. Numerical results show that RM and RM-polar codes with dynamic frozen bits of block length  $N \in \{128, 256\}$ , e.g., polarization-adjusted convolutional (PAC) codes [30] and dRM-polar codes, perform within 0.25 dB of the random-coding union (RCU) bound [44] with an average complexity very close to that of SC decoding at a frame error rate (FER) of  $10^{-5}$  or below. For higher FERs, the gap to the RCU bound is even smaller but with higher complexity. An optimized threshold test that limits attention to codeword candidates satisfying the threshold improves the performance when a maximum complexity constraint is imposed. In addition, the threshold test lets the decoder avoid making a decision [45] which provides simultaneous gains in overall FER and undetected frame error rate (uFER) for the (128, 64) PAC code as compared to a CRC-concatenated polar code under Successive cancellation list (SCL) decoding, where the CRC is optimized for the lower tail of the distance spectrum [29].

### A. Preview of the Proposed Algorithm

SCOS borrows ideas from SC-based flip [20], [21], sequential [14]–[17], [46] and list decoders [22], [47]–[49]. It is a tree search algorithm that flips the bits of valid paths to find a leaf with higher likelihood than other leaves, if such a leaf exists, and repeats until the ML decision is found. The search stores a list of branches that is updated progressively while running partial SC decoding by flipping the bits of the most likely leaf at each iteration. The order of the candidates is chosen according to the probability that they provide the ML decision. SCOS does not require an outer code (as for flip-decoders) or parameter optimization to optimize the performance vs. complexity trade-off (as for sequential decoders).

This paper is organized as follows. Section II gives background on the problem. Section III presents the SCOS algorithm with the pseudo codes. A lower bound on its complexity for ML decoding is described in Section IV. Section V presents numerical results and Section VI concludes the paper.

## II. PRELIMINARIES

Let  $x^a$  be the vector  $(x_1, x_2, \dots, x_a)$ ; if  $a = 0$ , then the vector is empty. Given  $x^N$  and a set  $\mathcal{A} \subset [N] \triangleq \{1, \dots, N\}$ ,

This work was supported by the German Research Foundation (DFG) under Grant KR 3517/9-1. This paper was presented in part at the IEEE Information Theory Workshop (ITW), October 2021, Kanazawa, Japan [1].

Peihong Yuan and Mustafa Cemil Coşkun are with the Institute for Communications Engineering (LNT), Technical University of Munich (TUM), Munich, Germany (email: {peihong.yuan,mustafa.coskun}@tum.de).

<sup>1</sup>RM codes achieve capacity over B-DMC under bit-wise ML decoding [7], i.e., the average bit error probability vanishes asymptotically in the block length.

<sup>2</sup>Long RM codes are not well-suited for SC decoding [9], [10]: the error probability of long RM codes under SC decoding is lower-bounded by  $1/2$  [2, Section X].

let  $x_{\mathcal{A}}$  be the subvector ( $x_i : i \in \mathcal{A}$ ). For sets  $\mathcal{A}$  and  $\mathcal{B}$ , the symmetric difference is denoted  $\mathcal{A} \triangle \mathcal{B}$  and an intersection set as  $\mathcal{A}^{(i)} \triangleq \mathcal{A} \cap [i]$ ,  $i \in [N]$ . Uppercase letters refer to random variables (RVs) and lowercase letters to realizations. A B-DMC is denoted as  $W : \mathcal{X} \rightarrow \mathcal{Y}$ , with input alphabet  $\mathcal{X} = \{0, 1\}$ , output alphabet  $\mathcal{Y}$ , and transition probabilities  $W(y|x)$  for  $x \in \mathcal{X}$  and  $y \in \mathcal{Y}$ . The transition probabilities of  $N$  independent uses of the same channel are denoted as  $W^N(y^N|x^N)$  and can be factored as  $W^N(y^N|x^N) = \prod_{i=1}^N W(y_i|x_i)$ . Capital bold letters refer to matrices, e.g.,  $\mathbf{B}_N$  denotes the  $N \times N$  *bit reversal* matrix [2] and  $\mathbf{G}_2$  denotes the  $2 \times 2$  Hadamard matrix.

#### A. $\mathbf{G}_N$ -coset Codes

Consider the matrix  $\mathbf{G}_N = \mathbf{B}_N \mathbf{G}_2^{\otimes n}$ , where  $N = 2^n$  with a non-negative integer  $n$  and  $\mathbf{G}_2^{\otimes n}$  is the  $n$ -fold Kronecker product of  $\mathbf{G}_2$ . For the set  $\mathcal{A} \subseteq [N]$  with  $|\mathcal{A}| = K$ , let  $U_{\mathcal{A}}$  have entries that are independent and identically distributed (i.i.d.) uniform *information* bits, and let  $U_{\mathcal{A}^c} = u_{\mathcal{A}^c}$  be fixed or *frozen*. The mapping  $c^N = u^N \mathbf{G}_N$  defines a  $\mathbf{G}_N$ -coset code [2]. Polar and RM codes are  $\mathbf{G}_N$ -coset codes with different selections of  $\mathcal{A}$  [2], [3].

Using  $\mathbf{G}_N$ , the transition probability from  $u^N$  to  $y^N$  is  $W_N(y^N|u^N) \triangleq W^N(y^N|u^N \mathbf{G}_N)$ . The transition probabilities of the  $i$ -th *bit-channel*, a synthesized channel with the input  $u_i$  and the output  $(y^N, u^{i-1})$ , are defined by

$$W_N^{(i)}(y^N, u^{i-1}|u_i) \triangleq \sum_{u_{i+1}^N \in \mathcal{X}^{N-i}} \frac{1}{2^{N-1}} W_N(y^N|u^N). \quad (1)$$

An  $(N, K)$  polar code is designed by placing the  $K$  most reliable bit-channels with indices  $i \in [N]$  into the set  $\mathcal{A}$  that can, e.g., be found using density evolution [2], [50]. An  $r$ -th order RM code of length- $N$  and dimension  $K = \sum_{i=0}^r \binom{n}{i}$ , where  $0 \leq r \leq n$ , is denoted as  $\text{RM}(r, n)$ . Its set  $\mathcal{A}$  consists of the indices,  $i \in [N]$ , with Hamming weight at least  $n - r$  for the binary expansion of  $i - 1$ . For both codes, one sets  $u_i = 0$  for  $i \in \mathcal{A}^c$ .

We make use of *dynamic* frozen bits [23]. A frozen bit is dynamic if its value depends on a subset of information bits preceding it; the resulting codes are called modified  $\mathbf{G}_N$ -coset codes. Dynamic frozen bits tend to improve the performance of near-ML decoders [10], [29]–[32] because the weight spectrum of the resulting code tends to improve as compared to the underlying code [29], [32]–[35], [37].

#### B. Related Decoding Algorithms

1) *Successive Cancellation Decoding*: Let  $c^N$  and  $y^N$  be the transmitted and received words, respectively. An SC decoder mimics an ML decision for the  $i$ -th bit-channel sequentially from  $i = 1$  to  $i = N$  as follows. For  $i \in \mathcal{F}$  set  $\hat{u}_i$  to its (dynamic) frozen value. For  $i \in \mathcal{A}$  compute the soft message  $\ell_i(\hat{u}_1^{i-1})$  defined as

$$\ell_i(\hat{u}_1^{i-1}) \triangleq \log \frac{P_{U_i|Y^N U^{i-1}}(0|y^N, \hat{u}_1^{i-1})}{P_{U_i|Y^N U^{i-1}}(1|y^N, \hat{u}_1^{i-1})} \quad (2)$$

by assuming that the previous decisions  $\hat{u}_1^{i-1}$  are correct and the frozen bits after  $u_i$  are uniformly distributed. Now make the hard decision

$$\hat{u}_i = \begin{cases} 0 & \text{if } \ell_i(\hat{u}_1^{i-1}) \geq 0 \\ 1 & \text{otherwise.} \end{cases} \quad (3)$$

Any erroneous decision  $\hat{u}_i \neq u_i$ ,  $i \in \mathcal{A}$ , cannot be corrected by SC decoding and results in a frame error. In the following, we review techniques to overcome this problem.

2) *Successive Cancellation List Decoding*: SCL decoding tracks several SC decoding paths [22] in parallel. At each decoding phase  $i \in \mathcal{A}$ , instead of making a hard decision on  $u_i$ , two possible decoding paths are continued in parallel threads. The maximum number  $2^k$  of paths implements ML decoding but with exponential complexity in  $k$ . To limit complexity, one may keep up to  $L$  paths at each phase. The reliability of decoding path  $v^i$  is quantified by a *path metric* (PM) defined as [51]

$$M(v^i) \triangleq -\log P_{U^i|Y^N}(v^i|y^N) \quad (4)$$

$$= M(v^{i-1}) + \log \left( 1 + e^{-(1-2v_i)\ell_i(v^{i-1})} \right) \quad (5)$$

$$\approx \begin{cases} M(v^{i-1}), & \text{if } \text{sign}(\ell_i(v^{i-1})) = 1 - 2v_i \\ M(v^{i-1}) + |\ell_i(v^{i-1})|, & \text{otherwise} \end{cases} \quad (6)$$

where (6) can be computed recursively using SC decoding with  $M(v^0) \triangleq 0$ . At the end of  $N$ -th decoding phase, a list  $\mathcal{L}$  of paths is collected. Finally, the output is the bit vector minimizing the PM:

$$\hat{u}^N = \underset{v^N \in \mathcal{L}}{\text{argmin}} M(v^N). \quad (7)$$

3) *Flip Decoding*: successive cancellation flip (SCF) decoding [20] aims to correct the first erroneous bit decision by sequentially flipping the unreliable decisions. This procedure requires an error-detecting outer code, e.g., a CRC code.

The SCF decoder starts by performing SC decoding for the inner code to generate the first estimate  $v^N$ . If  $v^N$  passes the CRC test, it is declared as the output  $\hat{u}^N = v^N$ . If not, then the SCF algorithm attempts to correct the bit errors at most  $T_{\max}$  times. At the  $t$ -th attempt,  $t \in [T_{\max}]$ , the decoder finds the index  $i_t$  of the  $t$ -th least reliable decision in  $v^N$  according to the amplitudes of the soft messages (2). The SCF algorithm restarts the SC decoder by flipping the estimate  $v_{i_t}$  to  $v_{i_t} \oplus 1$ . The CRC is checked after each attempt. This decoding process continues until the CRC passes or  $T_{\max}$  is reached.

Introducing a bias term to account for the reliability of the previous decisions enhances the performance [21]. The improved metric is calculated as

$$Q(i) = |\ell_i(v^{i-1})| + \sum_{j \in \mathcal{A}^{(i)}} \frac{1}{\alpha} \log \left( 1 + e^{-\alpha |\ell_j(v^{j-1})|} \right) \quad (8)$$

where  $\alpha > 0$  is a scaling factor.

SCF decoding can be generalized to flip multiple bit estimates at once, leading to dynamic successive cancellation flip

(DSCF) decoding [21]. The reliability of the initial estimates  $\tilde{u}_\mathcal{E}$ ,  $\mathcal{E} \subseteq \mathcal{A}$ , is described by

$$Q(\mathcal{E}) = \sum_{i \in \mathcal{E}} |\ell_i(v^{i-1})| + \sum_{j \in \mathcal{A}^{(i_{\max})}} \frac{1}{\alpha} \log(1 + e^{-\alpha |\ell_j(v^{j-1})|}) \quad (9)$$

where  $i_{\max}$  is the largest element in  $\mathcal{E}$ . The set of flipping positions is chosen as the one minimizing the metric (9) and is constructed progressively.

4) *Sequential Decoding*: We review two sequential decoding algorithms, namely successive cancellation stack (SCS) decoding [14]–[16] and successive cancellation Fano (SC-Fano) decoding [17], [30].

SCS decoding stores the  $L$  most reliable paths (possibly) with different lengths and discards the rest whenever the stack is full. At each iteration, the decoder selects the most reliable path and creates two possible decoding paths based on this path. The winning word is declared once a path length becomes  $N$ . SC-Fano decoding deploys a Fano search [46] that allows backward movement in the decoding tree and that uses a dynamic threshold. The dynamic threshold is initialized as  $T = 0$ . During the Fano search, if one cannot find a path with score less than  $T$  then the dynamic threshold is updated to  $T + \Delta$ , where  $\Delta$  is called the threshold spacing and controls the performance vs. complexity tradeoff.

Sequential decoding compares paths of different lengths. However, the probabilities  $P_{U^i|Y^N}(v^i|y^N)$ ,  $v^i \in \{0, 1\}^i$ , cannot capture the effect of the path's length. A new score is introduced in [16], [17] to account for the expected error rate of the future bits as

$$S(v^i) \triangleq -\log \frac{P_{U^i|Y^N}(v^i|y^N)}{\prod_{j=1}^i (1 - p_j)} \quad (10)$$

$$= M(v^i) + \sum_{j=1}^i \log(1 - p_j) \quad (11)$$

where  $p_j$  is the probability of the event that the first bit error occurred for  $u_j$  in SC decoding. The probabilities  $p_i$  can be computed via Monte Carlo simulation [2], [3] or they can be approximated via density evolution [50] offline. In the following, one may generalize the score as

$$S(v^i) = M(v^i) + b_i \quad (12)$$

where  $b_i$  is called a bias term. We discuss in Section V-A how the bias term affects the proposed decoding algorithm.

### III. SC ORDERED SEARCH DECODING

SCOS uses the metrics (6) and (10). We first define

$$\overline{M}(v^i) \triangleq M(v^{i-1}\overline{v}_i) = -\log P_{U^i|Y^N}(v^{i-1}\overline{v}_i|y^N) \quad (13)$$

$$\overline{S}(v^i) \triangleq \overline{M}(v^i) + b_i \quad (14)$$

where one may choose  $b_i$  as the second term in the right hand side (RHS) of (11).

Figure 1 shows an example of the decoding for  $N = 4$  and  $K = 4$ . SCOS starts by SC decoding to provide an output  $v^N$  as the current most likely leaf, e.g., the black path (0111) in Figure 1. This initial SC decoding computes and also stores the

PM  $\overline{M}(v^i)$  and the score  $\overline{S}(v^i)$  associated with the flipped versions of the decisions  $v_i$  for all  $i \in \mathcal{A}$ , e.g., illustrated as the red paths in Figure 1. Every index  $i \in \mathcal{A}$  with  $\overline{M}(v^i) < M(v^N)$  is a flipping set.<sup>3</sup> The collection of all flipping sets forms a list  $\mathcal{L}$  and each list member is visited in ascending order according to its score.

Upon deciding on a flipping set  $\mathcal{E}$  in the list  $\mathcal{L}$ , let index  $j \in [N]$  be the deepest common node of the current most likely leaf and the branch node defined by  $\mathcal{E}$  in the decoding tree (see the brown dot in Figure 1(a)). The decoder now flips the decision  $v_j$  and SC decoding continues. The set  $\mathcal{E}$  is popped from the list  $\mathcal{L}$ . The PMs (6) and scores (10) are calculated again for the flipped versions for decoding phases with  $i > j$ ,  $i \in \mathcal{A}$ , and the list  $\mathcal{L}$  is enhanced by new flipping sets progressively (similar to [21]). The branch node, including all of its child nodes, is discarded if at any decoding phase its PM exceeds that of the current most likely leaf, i.e.,  $M(v^N)$ .<sup>4</sup> Such a branch cannot output the ML decision, since for any valid path  $v^i$  the PM (6) is non-decreasing for the next stage, i.e., we have

$$M(v^i) \leq M(v^{i+1}), \forall v_{i+1} \in \{0, 1\}. \quad (15)$$

For instance, suppose that  $M(11) > M(0111)$  in Figure 1(g). Then any path  $\tilde{v}^N$  with  $\tilde{v}^2 = (1, 1)$  cannot be the ML decision; hence, it is pruned. If a leaf with lower PM is found, then it replaces the current most likely leaf. The procedure is repeated until one cannot find a more reliable path by flipping decisions, i.e., until  $\mathcal{L} = \emptyset$ . Hence, SCOS decoding implements an ML decoder.

Let  $\lambda(y^N)$  be the *number of node-visits* in the decoding tree by SCOS decoding (see Figure 1) for channel output  $y^N$ . The computational complexity of SCOS decoding can be limited by imposing a constraint on  $\lambda(y^N)$ , e.g.,  $\lambda(y^N) \leq \lambda_{\max}$ , at the expense of suboptimality. To also limit the space complexity, one can impose a list size, e.g., we relate the space complexity to the number of node-visits heuristically as

$$|\mathcal{L}| \leq \eta \triangleq \log_2 N \times \frac{\lambda_{\max}}{N}. \quad (16)$$

#### A. Detailed Description

This section provides pseudo code<sup>5</sup> and the details of the proposed SCOS decoder. The required data structures together with their size are listed in Table I. Note that arrays  $\mathbb{L}$  and  $\mathbb{C}$  both store  $(\log_2 N + 1) \times N$  elements, in contrast to [22] where only  $2N - 1$  elements are stored, since we reuse some decoding paths to decrease the computational complexity (similar to the SC-Fano decoder). In the pseudo code, the notation  $\mathbb{v}[i]$  refers to the  $i$ -th entry of an array  $\mathbb{v}$ . Similarly, the entry in position  $(i, j)$  of array  $\mathbb{C}$  is denoted as  $\mathbb{C}[i, j]$ . The entries of bias vector  $\mathbb{b}$  are computed offline via

$$\mathbb{b}[i] = \sum_{j=1}^i \log(1 - p_j), \quad i \in [N] \quad (17)$$

<sup>3</sup>Each set is a singleton at this stage.

<sup>4</sup>This pruning method is similar to the adaptive skipping rule proposed in [49] for ordered-statistics decoding [47], [48].

<sup>5</sup>In the pseudo code, we use type-writer font for the data structures (with an exception for sets) and 1-based indexing arrays.

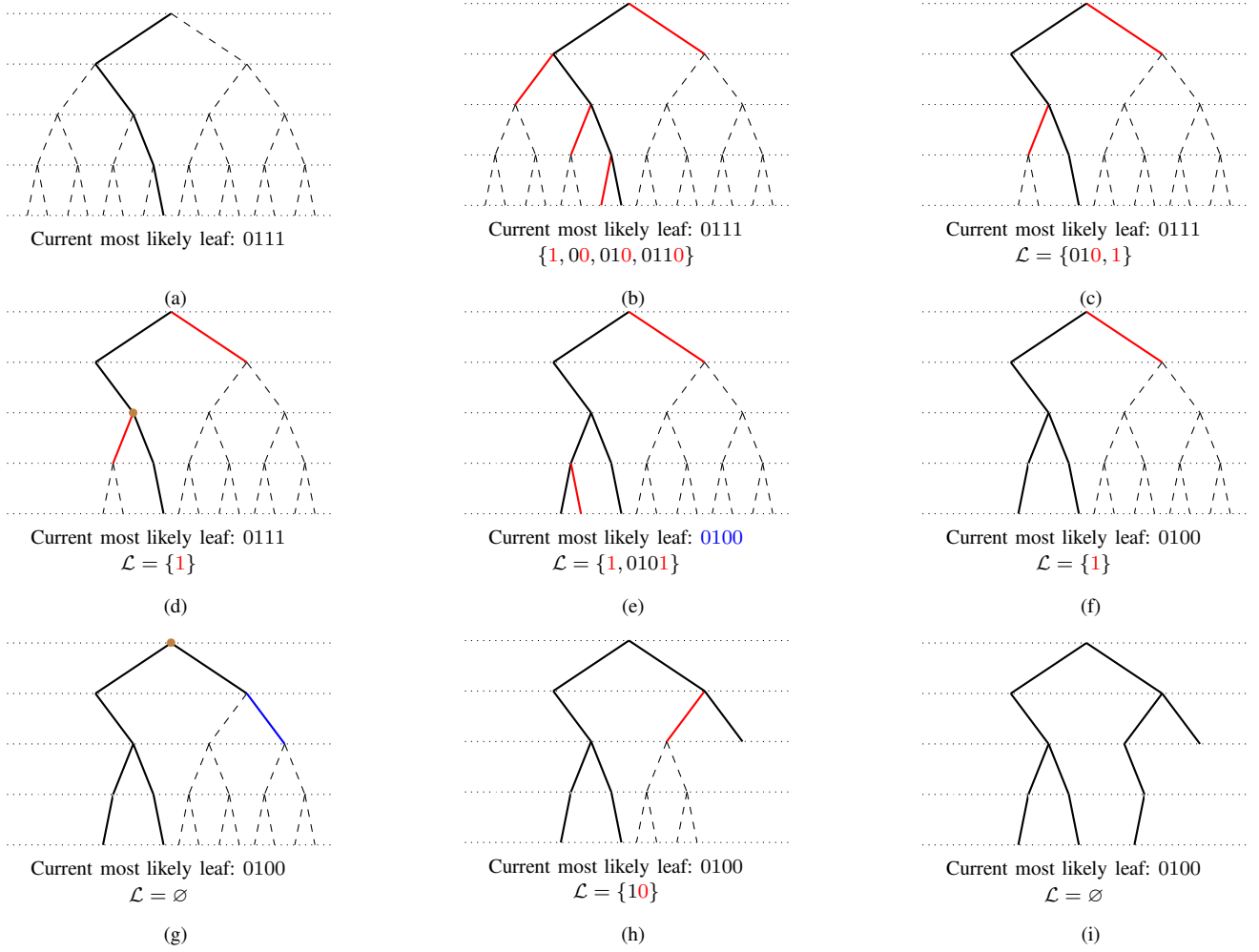


Fig. 1: (a) Initial SC decoding outputs  $v^N = (0111)$  with the corresponding PM  $M(v^N)$ . (b) During the initial SC decoding, the PMs and scores are computed for branch nodes  $\{1, 00, 010, 0110\}$ . (c) The branch nodes with PMs larger than that of the current most likely leaf are pruned, e.g., we have  $M(00), M(0110) > M(0111)$ . Suppose now that  $S(010) < S(1)$  and the members of  $\mathcal{L}$  are ordered in the ascending order according to their scores. (d) The first candidate is popped from the list and the decoder returns to the deepest (or nearest) common node. (e) The decision is flipped and SC decoding continues. During decoding, the list  $\mathcal{L}$  and the current most likely leaf are updated. (f) The branch nodes with PMs larger than that of the current most likely leaf are pruned as in (c) (in this case, a leaf node is removed). (g) Repeat the procedure as in step (d), where we assume  $M(11) > M(0100)$ . (h) The list  $\mathcal{L}$  is updated when the branch (11) was visited. (i) The decoder examines the last member of the list  $\mathcal{L}$  and pops it from  $\mathcal{L}$ . After reaching the  $N$ -th decoding phase, suppose that there is no branch node left, which has a smaller PM than that of the current most likely leaf, i.e.,  $\mathcal{L} = \emptyset$ . The current most likely leaf is declared as the decision  $\hat{u}^N$ .

---

**Algorithm 1:** InsertList( $\mathcal{F}$ )

---

**Input :** structure  $\mathcal{F}$  of a flipping set

```

1  $i = |\mathcal{L}| + 1$ 
2 while  $i > 1$  and  $\mathcal{F}.\overline{S}_{\mathcal{E}} < \mathcal{L}[i-1].\overline{S}_{\mathcal{E}}$  do
3    $i = i - 1$ 
4 insert  $\mathcal{F}$  in list  $\mathcal{L}$  at position  $i$ 
5 if  $|\mathcal{L}| > \eta$  then
6   pop the last element of  $\mathcal{L}$ 
```

---

unless otherwise stated.

A list  $\mathcal{L}$  containing flipping structures  $\mathcal{F} = \langle \mathcal{E}, \overline{M}_{\mathcal{E}}, \overline{S}_{\mathcal{E}} \rangle$  is constructed,<sup>6</sup> where  $\mathcal{E}$  is the set of flipping indices. Then  $\overline{M}_{\mathcal{E}}$  and  $\overline{S}_{\mathcal{E}}$  are the respective path metric and the score function associated to the flipping set  $\mathcal{E}$ , as defined in (13) and (14).

<sup>6</sup>Observe that the list in Figure 1 is slightly different for simplicity.

---

**Algorithm 2:** FindStartIndex( $\mathcal{E}, \mathcal{E}_p$ )

---

**Input :** flipping sets  $\mathcal{E}$  and  $\mathcal{E}_p$

**Output:** first different index

```

1 for  $i = 1, 2, \dots, N$  do
2   if  $(i \in \mathcal{E}) \oplus (i \in \mathcal{E}_p)$  then
3     return  $i$ 
```

---

The size of  $\mathcal{L}$  is constrained by a user-defined parameter  $\eta$ , e.g., a good choice is given in (16). Algorithm 1 is used to insert a new member into the list and the members are stored in ascending order according to their score, i.e., for any pair of  $i$  and  $j$  such that  $1 \leq i < j \leq \eta$  we have  $\mathcal{L}[i].\overline{S}_{\mathcal{E}} \leq \mathcal{L}[j].\overline{S}_{\mathcal{E}}$ . Given two flipping sets, Algorithm 2 finds the decoding stage to which the decoder should return, see Figure 1(d).

Algorithm 3 is a modified SC decoder, where the modifica-

TABLE I  
DATA STRUCTURES FOR SCOS DECODING.

name	size	data type	description
$b$	$N$	float	precomputed bias term
$L$	$(\log_2 N + 1) \times N$	float	log-likelihood ratio (LLR)
$C$	$(\log_2 N + 1) \times N$	binary	hard decision
$\hat{u}, v$	$N$	binary	decoding path
$M, \bar{M}, \bar{S}$	$N$	float	metric
$M_{\text{cml}}$	1	float	PM of the current most likely leaf
$\mathcal{E}, \mathcal{E}_p$	1	set (of indices)	flipping set
$F$	1	$\langle \text{set, float, float} \rangle$	structure of a flipping set
$\mathcal{L}$	$\leq \eta$	type of $F$	list of flipping structures

---

**Algorithm 3:** SCDec ( $i_{\text{start}}, \mathcal{E}$ )

---

**Input :** start index  $i_{\text{start}}$ , flipping set  $\mathcal{E}$   
**Output:** end index  $i_{\text{end}}$

```

1  $m = \log_2 N$ 
2 for  $i = i_{\text{start}}, \dots, N$  do
3   recursivelyCalcL ( $m + 1, i - 1$ )
4   if  $i \notin \mathcal{A}$  then
5      $v[i] = 0$  // compute  $v[i]$  if
       dynamically frozen
6   else
7     if  $i \in \mathcal{E}$  then
8        $v[i] = \text{HardDec}(L[m + 1, i]) \oplus 1$ 
9     else
10       $v[i] = \text{HardDec}(L[m + 1, i])$ 
11     if  $i > \text{maximum}(\mathcal{E})$  then
12        $\bar{M}[i] =$ 
13       CalcPM ( $M[i - 1], v[i] \oplus 1, L[m + 1, i]$ )
14        $\bar{S}[i] = \bar{M}[i] + b[i]$ 
15      $M[i] = \text{CalcPM}(M[i - 1], v[i], L[m + 1, i])$ 
16     if  $M[i] \geq M_{\text{cml}}$  then
17       return  $i$ 
18    $C[m + 1, i] = v[i]$ 
19   if  $i \bmod 2 = 0$  then
20     recursivelyCalcC ( $m + 1, i - 1$ )
21 if  $M[N] < M_{\text{cml}}$  then
22    $M_{\text{cml}} = M[N]$ 
23   for  $i = 1, 2, \dots, N$  do
24      $\hat{u}[i] = v[i]$ 
25   return  $N$ 

```

---

tions are highlighted as blue in the pseudo code.

- One can start at any decoding phase  $i_{\text{start}}$ . The starting index  $i_{\text{start}}$  is found by Algorithm 2 which returns the first index that differs between the current and previous flipping sets.
- Algorithm 3 keeps updating the PM  $M$  (line 14).
- The decisions are flipped at the decoding phases in  $\mathcal{E}$  (line 7-9).

---

**Algorithm 4:** SCOS ( $\ell^N$ )

---

**Input :** LLRs  $\ell^N$   
**Output:** estimates  $\hat{u}$

```

1  $\mathcal{L} = \emptyset, \mathcal{E}_p = \emptyset, M_{\text{cml}} = +\infty$ 
2 for  $i = 1, 2, \dots, N$  do
3    $L[1, i] = \ell_i$ 
4   SCDec ( $1, \emptyset$ )
5   for  $i = 1, 2, \dots, N$  do
6     if  $i \in \mathcal{A}$  and  $\bar{M}[i] < M_{\text{cml}}$  then
7       InsertList ( $\langle \{i\}, \bar{M}[i], \bar{S}[i] \rangle$ )
8   while  $\mathcal{L} \neq \emptyset$  do
9      $\langle \mathcal{E}, \bar{M}_{\mathcal{E}}, \bar{S}_{\mathcal{E}} \rangle = \text{popfirst}(\mathcal{L})$  // pop the first
       element of  $\mathcal{L}$ 
10    if  $\bar{M}_{\mathcal{E}} < M_{\text{cml}}$  then
11       $i_{\text{start}} = \text{FindStartIndex}(\mathcal{E}, \mathcal{E}_p)$ 
12       $i_{\text{end}} = \text{SCDec}(i_{\text{start}}, \mathcal{E})$ 
13      for  $i = \text{maximum}(\mathcal{E}) + 1, \dots, i_{\text{end}}$  do
14        if  $i \in \mathcal{A}$  and  $\bar{M}[i] < M_{\text{cml}}$  then
15          InsertList ( $\langle \mathcal{E} \cup \{i\}, \bar{M}[i], \bar{S}[i] \rangle$ )
16       $\mathcal{E}_p = \mathcal{E}$ 
17 return  $\hat{u}$ 

```

---

- Algorithm 3 uses the values  $\bar{M}[i]$  and  $\bar{S}[i]$  for  $i \in \mathcal{A}, i > \text{maximum}(\mathcal{E})$  (line 11-13).
- If a more likely leaf (i.e., a path of length- $N$ ) is found, update  $\hat{u}$  and  $M_{\text{cml}}$  (line 20-23).
- If the PM  $M[i]$  is larger than  $M_{\text{cml}}$ , stop SCDec function and return the current phase  $i$  as  $i_{\text{end}}$  (line 15-16).

Note that the function CalcPM (lines 12 and 14) takes a real-valued PM, a binary decision and a real-valued LLR as inputs and updates the PM using (6).

Algorithm 4 is the main loop of the SCOS decoder. The metric  $M_{\text{cml}}$  is initialized to  $+\infty$ . After the initial SC decoding (line 4),  $M_{\text{cml}}$  is updated to the PM of the SC estimate. Then a tree search is performed, where the candidates are ordered by their score functions  $\bar{S}$ . Many sub-trees are pruned because of the threshold  $M_{\text{cml}}$ , i.e., the PM of the current most likely leaf. The stopping condition of the “while loop” (line 8

with  $\mathcal{L} = \emptyset$ ) implies that the most likely codeword is found, i.e., there cannot be any other codeword with a smaller PM. The estimate corresponding to  $M_{\text{cm1}}$  is output as the decision.

**Remark 1.** SCOS stores only the flipping set and the corresponding metrics in  $\mathcal{L}$ . Alternatively, one may store the memory of all decoding paths in  $\mathcal{L}$  as for SCS decoding [15], [16] to prevent node-revisits, which trades memory requirement for computational complexity. The size of the arrays  $L$  and  $C$  is then increased to  $\eta \times (2N - 1)$ .

#### IV. COMPLEXITY FOR ML DECODING

The decoding complexity is measured by the *number of node-visits*. For instance, the number  $\lambda_{\text{SC}}$  of node-visits for SC decoding is simply the code length  $N$  independent of the channel output  $y^N$ . For a given code construction, the number  $\lambda_{\text{SCL}}(L, \mathcal{A})$  of node-visits for SCL decoding with list size  $L$  is also constant and upper bounded as  $\lambda_{\text{SCL}}(L, \mathcal{A}) \leq LN$ . On the other hand, the complexity  $\lambda(y^N)$  of SCOS decoding depends on the channel output as for other sequential decoders [52]; hence, it is a RV defined as  $\Lambda \triangleq \lambda(Y^N)$ . In the following, we are interested in the average behaviour of  $\Lambda$ .

To understand the minimum complexity of SCOS decoding, consider the set of partial input sequences  $v^i, i \in [N]$ , with a smaller PM than the ML decision  $\hat{u}_{\text{ML}}^N$ .<sup>7</sup>

**Definition 1.** For the channel output  $y^N$  and the binary sequence  $v^N \in \mathcal{X}^N$ , define the set

$$\mathcal{V}(v^N, y^N) \triangleq \bigcup_{i=1}^N \{u^i \in \{0, 1\}^i : M(u^i) \leq M(v^N)\}. \quad (18)$$

**Lemma 1.** We have

$$\lambda(y^N) \geq |\mathcal{V}(\hat{u}_{\text{ML}}^N(y^N), y^N)| \quad (19)$$

and the expected complexity is lower bounded as

$$\frac{1}{\lambda_{\text{SC}}} \mathbb{E}[\Lambda] \geq \frac{1}{N} \mathbb{E}[|\mathcal{V}(\hat{u}_{\text{ML}}^N(Y^N), Y^N)|]. \quad (20)$$

*Proof.* Inequality (19) follows from (18) by replacing  $v^N$  with the ML decision  $\hat{u}_{\text{ML}}^N$  and the description of SCOS decoding. Since (19) is valid for any  $y^N$ , the bound (20) follows by  $\lambda_{\text{SC}} = N$ .  $\square$

**Remark 2.** Recall that the PM (6) is calculated using the SC decoding schedule, i.e., it ignores the frozen bits coming after the current decoding phase  $i$ . This means the size of the set (18) tends to be smaller for codes more suited for SC decoding, e.g., polar codes, while it is larger for other codes such as RM codes. This principle is also observed when decoding via SCL decoding, i.e., the required list size to approach ML performance grows when one “interpolates” from polar to RM codes [10], [18], [19], [31]. This observation motivates the dRM-polar codes in Section V that provide a good performance vs. complexity trade-off under SCOS decoding for moderate code lengths, e.g.,  $N = 256$  bits.

<sup>7</sup>There are  $i$  node-visits for SC decoding for any decoding path  $v^i$ .

#### V. NUMERICAL RESULTS

This section provides simulation results for binary-input additive white Gaussian noise (biAWGN) channels. We provide FERs and complexities for modified  $G_N$ -coset codes under SCOS decoding with and without a maximum complexity constraint. The RCU and metaconverse (MC) bounds [44] are included as benchmarks. The empirical *ML lower bounds* of [22] are also plotted for the case of SCOS decoding with a maximum complexity constraint. Each time a decoding failure occurred the decision  $\hat{u}^N$  was checked if

$$M(\hat{u}^N) \leq M(u^N). \quad (21)$$

In this case, even an ML decoder would make an error.

Figure 2 shows the FER and complexity vs. signal-to-noise ratio (SNR) in  $E_b/N_0$  for a (128, 64) PAC code [30] under SCOS decoding. The complexity is normalized by the complexity of SC decoding. The information set  $\mathcal{A}$  is the same as that of the RM code, and the polynomial of the convolutional code is  $\mathbf{g} = (0, 1, 1, 0, 1, 1)$ . In other words, we use a modified RM code with dynamic frozen bits with the following constraints:

$$u_i = u_{i-2} \oplus u_{i-3} \oplus u_{i-5} \oplus u_{i-6}, \quad i \in \mathcal{F} \text{ and } i > 6. \quad (22)$$

The average complexity is large for (near-)ML decoding of RM codes with dynamic frozen bits, so we introduce dRM codes [10] as an ensemble of modified RM-polar codes.

**Definition 2.** The  $(N, K)$  dRM-polar ensemble is the set of codes specified by the set  $\mathcal{A}$  of an  $(N, K)$  RM-polar code and choosing

$$u_i = 0 \oplus \sum_{j \in \mathcal{A}^{(i-1)}} v_{j,i} u_j, \quad \forall i \in \mathcal{A}^c, \quad (23)$$

with all possible  $v_{j,i} \in \{0, 1\}$  and  $\mathcal{A}^{(0)} \triangleq \emptyset$ , where  $\sum$  denotes XOR summation.

Figure 3 shows simulation results for a rate  $R \approx 0.6$  and length  $N = 256$  dRM-polar code chosen randomly from this ensemble. We observe the following behavior in Figures 2 and 3.

- SCOS decoding with unbounded complexity matches the ML lower bound since it implements an ML decoder.
- The average complexity  $\mathbb{E}[\Lambda]$  of a SCOS decoder approaches the complexity of an SC decoder for low FERs ( $10^{-5}$  or below for the PAC code and around  $10^{-6}$  for the dRM-polar code). Indeed, it reaches the ultimate limit given by Lemma 1, which is not the case for SC-Fano decoding. The difference to the RCU bound [44] is at most 0.2 dB for the entire SNR regime for the PAC code and slightly larger for the dRM-polar code.
- The lower bound on the average given by (20) is validated and is tight for high SNR. However, the bound appears to be loose at low SNR values mainly for two reasons: (i) usually the initial SC decoding estimate  $v^N$  is not the ML decision and extra nodes in the difference set  $\mathcal{V}(v^N, y^N) \setminus \mathcal{V}(\hat{u}_{\text{ML}}^N, y^N)$  are visited and (ii) SCOS decoding visits the same node multiple times and this cannot be tracked by a set definition. These revisits prevent us

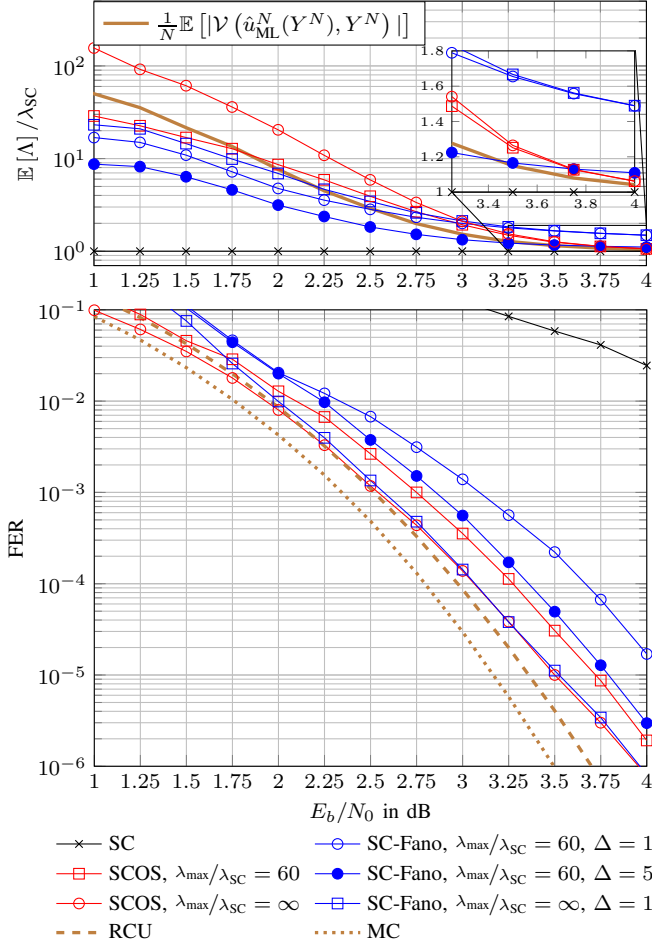


Fig. 2: FER/average number of node visits (normalized by  $N$ ) vs.  $E_b/N_0$  over the biAWGN channel for a (128, 64) PAC code with the information set  $\mathcal{A}$  of RM(3, 7) code and the polynomial  $g = (0, 1, 1, 0, 1, 1)$  under SCOS decoding, compared to SC-Fano decoding.

from providing an upper bound for the complexity, which could have been interesting for the regime where the lower bound is loose. Nevertheless, it may be possible to reduce the number of revisits by improving the search schedule.

- A parameter  $\Delta$  must be optimized carefully for SC-Fano decoding to achieve ML performance and this usually requires extensive simulations. A small  $\Delta$  and no complexity constraint would also approach ML performance; however, the complexity explodes for longer codes. As seen from Figure 2,  $\Delta = 1$  matches ML performance but the average complexity is almost double that of SC decoding near or below FERs of  $10^{-5}$ . Moreover, under a maximum-complexity constraint, the average complexity of SC-Fano decoding is not closer than SCOS decoding to that of SC decoding for similar performance.
- The parameter  $\Delta$  must be optimized again for a good performance once a maximum-complexity constraint is imposed. Otherwise, the performance degrades significantly. Even so, SCOS decoding outperforms SC-Fano decoding for the same maximum-complexity constraint. However, SC-Fano decoding has a lower average complexity for high FERs (if  $\Delta$  is optimized) with a degradation in the performance. In contrast, SCOS decoding does not

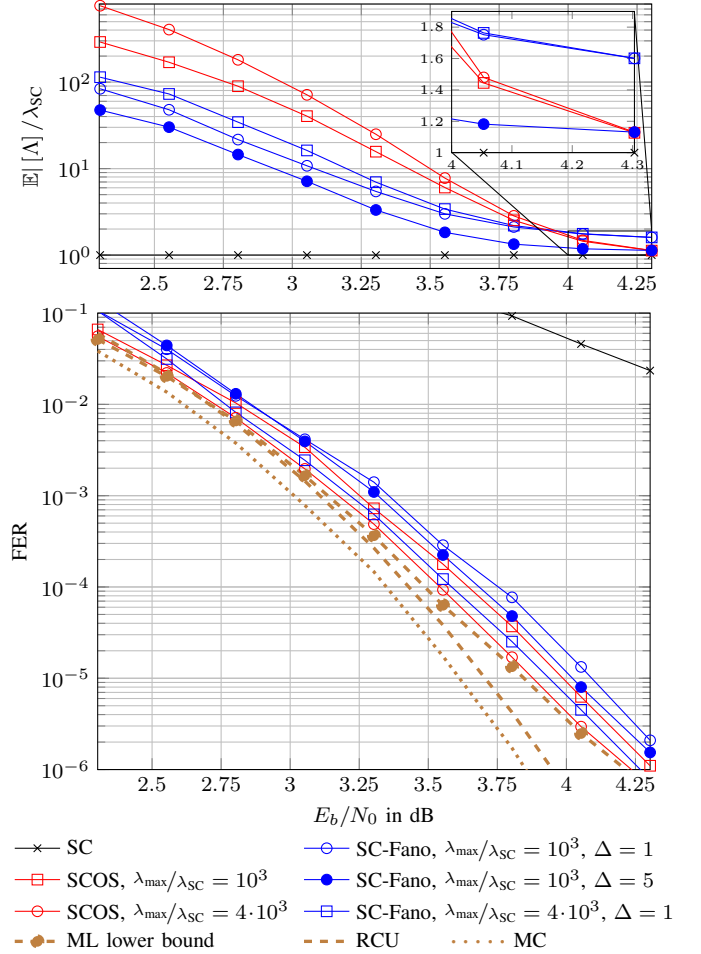


Fig. 3: FER/average number of node visits (normalized by  $N$ ) vs.  $E_b/N_0$  over the biAWGN channel for a (256, 154) dRM-polar code under SCOS decoding, compared to SC-Fano decoding. The information set  $\mathcal{A}$  is constructed as in [18] where the mother code is the RM(4, 8) and the polar rule is given by setting  $\beta = 2^{1/4}$  in [53].

require such an optimization.

#### A. Bias Term Robustness

Consider the bias terms  $b_i$  given in (12), which impacts the search priority but not the performance. This means that a *suboptimal* bias term does not change the performance of SCOS decoding with unbounded complexity (which is still ML), but increases its complexity. Figure 4 illustrates the effect of various bias terms outlined below on the performance of SCOS decoding.

- The bias terms are computed via the RHS of (17) using density evolution for each SNR point.
- The bias terms are set to zero, i.e.,  $b_i = 0$ ,  $i \in [N]$ .

As mentioned above, the changes in the bias terms do not affect the performance if there is no complexity constraint. The complexity reduction is limited if (17) is used instead of setting the bias terms to zero. Nevertheless, setting them to zero slightly degrades the performance (by  $\approx 0.12$  dB) when the maximum complexity is constraint to five times that of SC decoding with almost no savings in the average complexity. Hence, we conclude that SCOS decoding is not very sensitive to the choice of bias terms.



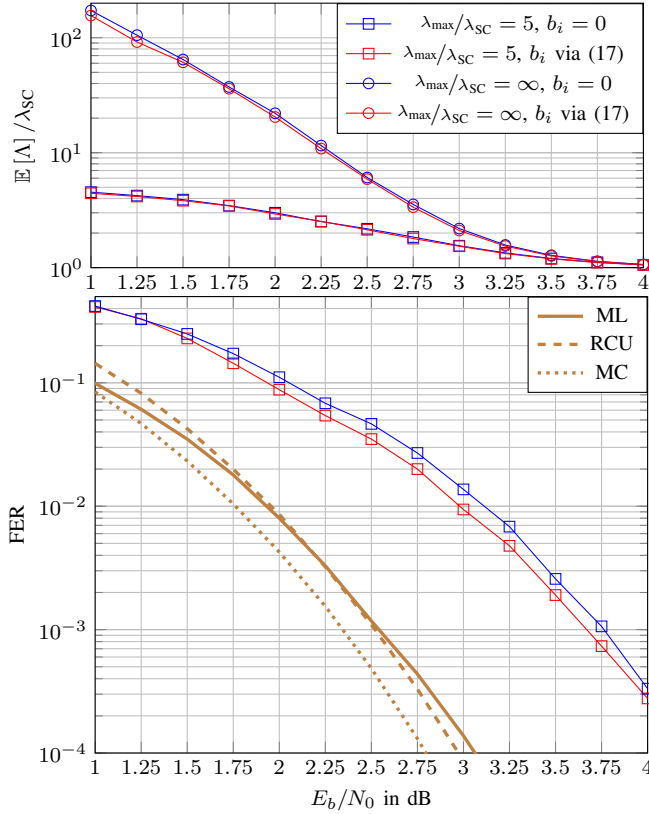


Fig. 4: FER/average number of node visits (normalized by  $N$ ) vs.  $E_b/N_0$  over the biAWGN channel for a  $(128, 64)$  PAC code with the information set  $\mathcal{A}$  of RM(3, 7) code and the polynomial  $\mathbf{g} = (0, 1, 1, 0, 1, 1)$  under SCOS decoding with various bias terms and maximum complexity constraints.

### B. Further Improvements

Monte Carlo simulation and genie-aided SC decoding [2] can be used to approximate the probability density function (PDF) of the PM for the transmitted message at a given SNR.<sup>8</sup> Figure 5 provides the PDF for the  $(128, 64)$  PAC code at  $E_b/N_0 = 3.5$  dB. Observe that  $\Pr(M(u^N) > 50) \approx 0$ , i.e., if the decoder discards the paths having PMs larger than 50 then the performance degradation is negligible while reducing computational complexity. Such a modification is particularly relevant when a maximum complexity constraint is imposed on SCOS decoding. In this case, unnecessary node-visits drain the computation budget and increase the number of suboptimal decisions. Moreover, the threshold test lets the decoder reject unreliable decisions and reduces the number of undetected errors if the threshold is carefully optimized, see [45].

In the following, we modify SCOS decoding by setting a maximum PM  $M_{\max}$  as shown in Algorithm 5. Figure 6 compares the performance of the modified algorithm to that of conventional SCOS. The modified SCOS gains  $\approx 0.25$  dB with the same maximum complexity constraint  $\lambda_{\max} = 5N$  if  $M_{\max} = 35$ . Note that the average complexity is similar.

For a given threshold  $M_{\max}$ , define the binary RV

$$\Omega = \mathbb{1}\{M(\hat{u}^N) \leq M_{\max}\} \quad (24)$$

<sup>8</sup>Note that  $M(u^N)$  is a RV where the source of randomness is the channel output. Since we consider symmetric B-DMCs and a linear code with uniform distribution, the PDF of  $M(u^N)$  could be computed with an all zero codeword assumption.

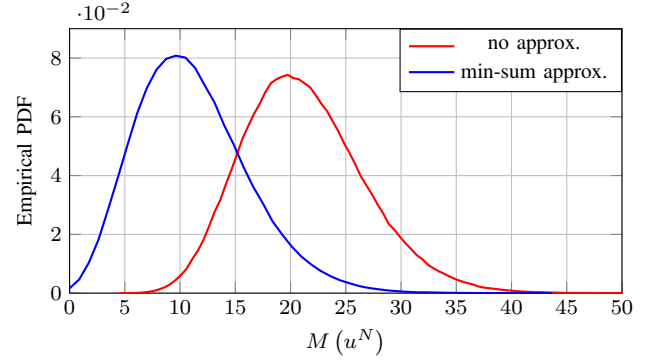


Fig. 5: Empirical PDF (via  $10^7$  samples) of the  $M(u^N)$  over the biAWGN channel at 3.5 dB SNR for a  $(128, 64)$  PAC code with the information set  $\mathcal{A}$  of RM(3, 7) code and the polynomial  $\mathbf{g} = (0, 1, 1, 0, 1, 1)$ . The blue line is obtained via genie-aided SC decoding [2] with min-sum approximation while the red line computes the PMs without any approximation.

### Algorithm 5: SCOS with maximum PM ( $\ell^N, M_{\max}$ )

---

**Input :** input LLRs  $\ell^N$ ,  $M_{\max}$   
**Output:** output vector  $\hat{u}$ , decoding state  $\omega$

---

```

1  $\mathcal{L} = \emptyset, \mathcal{E}_p = \emptyset, M_{\text{cml}} = M_{\max}, \omega = 0$ 
2 for  $i = 1, 2, \dots, N$  do
3    $\mathbb{L}[1, i] = \ell_i$ 
4  $i_{\text{end}} = \text{SCDec}(1, \emptyset)$ 
5 if  $i_{\text{end}} = N$  then  $\omega = 1$ 
6 for  $i = 1, 2, \dots, N$  do
7   if  $i \in \mathcal{A}$  and  $\bar{M}[i] < M_{\text{cml}}$  then
8      $\mathbb{L}[\text{InsertList}(\langle \{i\}, \bar{M}[i], \bar{\mathcal{S}}[i] \rangle)]$ 
9 while  $\mathcal{L} \neq \emptyset$  do
10   $\langle \mathcal{E}, \bar{M}_{\mathcal{E}}, \bar{\mathcal{S}}_{\mathcal{E}} \rangle = \text{popfirst}(\mathcal{L})$ 
11  if  $\bar{M}_{\mathcal{E}} < M_{\text{cml}}$  then
12     $i_{\text{start}} = \text{FindStartIndex}(\mathcal{E}, \mathcal{E}_p)$ 
13     $i_{\text{end}} = \text{SCDec}(i_{\text{start}}, \mathcal{E})$ 
14    if  $i_{\text{end}} = N$  then  $\omega = 1$ 
15    for  $i = \text{maximum}(\mathcal{E}) + 1, \dots, i_{\text{end}}$  do
16      if  $i \in \mathcal{A}$  and  $\bar{M}[i] < M_{\text{cml}}$  then
17         $\mathbb{L}[\text{InsertList}(\langle \mathcal{E} \cup \{i\}, \bar{M}[i], \bar{\mathcal{S}}[i] \rangle)]$ 
18     $\mathcal{E}_p = \mathcal{E}$ 
19 return  $\hat{u}, \omega$ 

```

---

where the indicator function  $\mathbb{1}\{P\}$  takes on the value 1 if the proposition  $P$  is true and 0 otherwise. The proposition of the indicator function (24) reads as “the modified SCOS decoding finds an estimate  $\hat{u}^N$  with a PM smaller than  $M_{\max}$ ”. The undetected error probability of the algorithm is

$$\Pr(\hat{U}^N \neq U^N, \Omega = 1). \quad (25)$$

The overall error probability is the sum of the detected and undetected error probabilities, i.e., we have

$$\Pr(\hat{U}^N \neq U^N) = \sum_{\omega \in \{0, 1\}} \Pr(\hat{U}^N \neq U^N, \Omega = \omega) \quad (26)$$

which follows from the law of total probability. The parameter  $M_{\max}$  controls the FER and uFER tradeoff [45], [54]. In particular, (25) is the left hand side (LHS) of (26) if



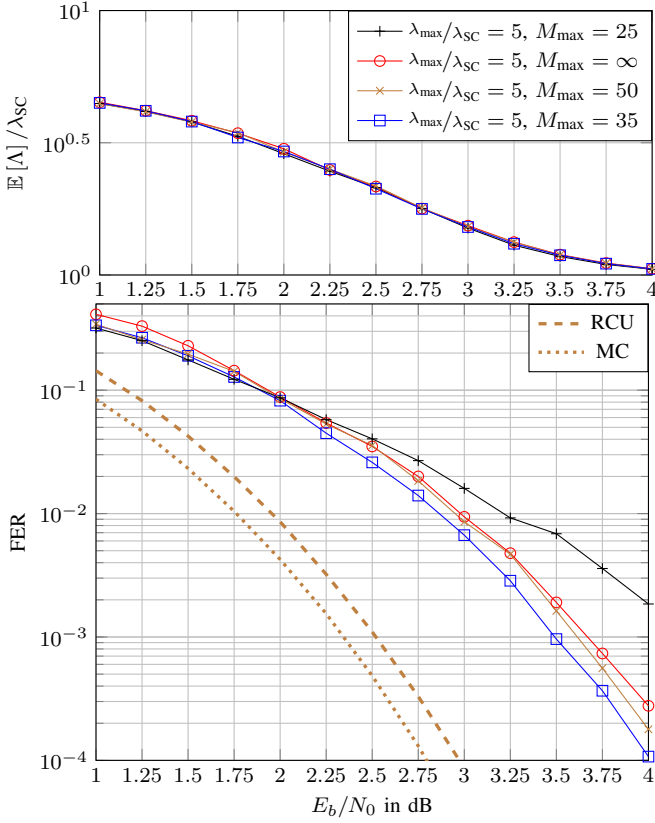


Fig. 6: FER/average number of node visits (normalized by  $N$ ) vs.  $E_b/N_0$  over the biAWGN channel for a (128, 64) PAC code with the information set  $\mathcal{A}$  of RM(3, 7) code and the polynomial  $\mathbf{g} = (0, 1, 1, 0, 1, 1)$  under modified SCOS decoding with various maximum PMs and a fixed maximum complexity constraint.

$M_{\max} = \infty$ . Figure 7 illustrates that the (128, 64) PAC code under modified SCOS decoding gains in overall FER and in uFER as compared to a (128, 71) polar code concatenated with a CRC-7 (resulting in a (128, 64) overall code) under SCL decoding with  $L = 16$  at high SNR. Furthermore, the code outperforms DSCF decoding with the maximum number  $T_{\max} = 70$  of bit flips although with a small increase in the average complexity.

## VI. CONCLUSIONS

The SCOS algorithm was proposed that implements ML decoding. The complexity adapts to the channel quality and approaches the complexity of SC decoding for polar codes and short RM codes at high SNR. Unlike existing alternatives, the algorithm does not need an outer code or a separate parameter optimization. A lower bound on the complexity is approached at high SNR.

SCOS was modified to limit the worst-case complexity and to provide a trade-off between the overall and undetected error probabilities. Using the modified SCOS, polar codes with dynamic frozen bits, e.g., a (128, 64) PAC code, provide simultaneous gains in the overall and undetected FERs and complexity as compared to CRC-concatenated polar codes under SCL decoding.

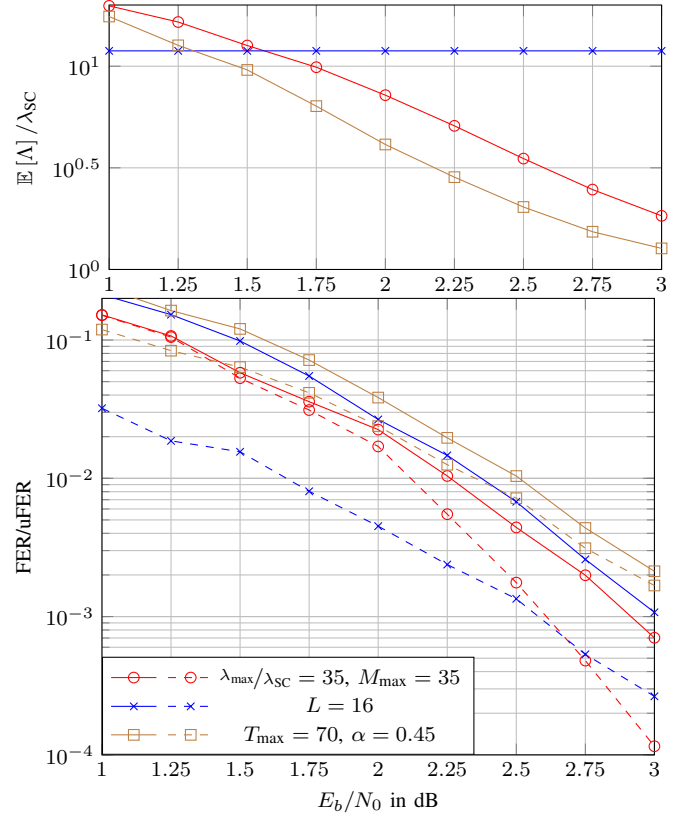


Fig. 7: FER/average number of node visits (normalized by  $N$ ) vs.  $E_b/N_0$  over the biAWGN channel for a (128, 64) PAC code with the information set  $\mathcal{A}$  of RM(3, 7) code and the polynomial  $\mathbf{g} = (0, 1, 1, 0, 1, 1)$  under modified SCOS decoding with a maximum PMs and a fixed maximum complexity constraint compared to a (128, 64) modified polar code with an outer CRC-7 having the generator polynomial  $g(x) = x^7 + x^6 + x^5 + x^2 + 1$  [29].

## ACKNOWLEDGEMENTS

The authors thank Gerhard Kramer (TUM) for discussions which motivated the work and for improving the presentation.

## REFERENCES

- [1] P. Yuan and M. C. Coşkun, "Complexity-adaptive maximum-likelihood decoding of modified  $\mathcal{G}_N$ -coset codes," in *IEEE Information Theory Workshop (ITW)*, Oct. 2021, pp. 1–6.
- [2] E. Arkan, "Channel polarization: A method for constructing capacity-achieving codes for symmetric binary-input memoryless channels," *IEEE Trans. Inf. Theory*, vol. 55, no. 7, pp. 3051–3073, Jul. 2009.
- [3] N. Stolte, "Rekursive Codes mit der Plotkin-Konstruktion und ihre Decodierung," Ph.D. dissertation, TU Darmstadt, 2002.
- [4] I. Reed, "A class of multiple-error-correcting codes and the decoding scheme," *Trans. IRE Prof. Group on Inf. Theory*, vol. 4, no. 4, pp. 38–49, Sep. 1954.
- [5] D. E. Muller, "Application of boolean algebra to switching circuit design and to error detection," *Trans. IRE Prof. Group on Electronic Computers*, vol. EC-3, no. 3, pp. 6–12, Sep. 1954.
- [6] S. Kudekar, S. Kumar, M. Mondelli, H. D. Pfister, E. Şaşıoğlu, and R. L. Urbanke, "Reed-Muller codes achieve capacity on erasure channels," *IEEE Trans. Inf. Theory*, vol. 63, no. 7, pp. 4298–4316, Jul. 2017.
- [7] G. Reeves and H. D. Pfister, "Reed-muller codes achieve capacity on BMS channels," *CoRR*, vol. abs/2110.14631, 2021. [Online]. Available: <http://arxiv.org/abs/2110.14631>
- [8] M. C. Coşkun, G. Durisi, T. Jerkovits, G. Liva, W. Ryan, B. Stein, and F. Steiner, "Efficient error-correcting codes in the short blocklength regime," *Elsevier Phys. Commun.*, vol. 34, pp. 66–79, Jun. 2019.
- [9] K. Ivanov and R. Urbanke, "On the efficiency of polar-like decoding for symmetric codes," *CoRR*, vol. abs/2104.06084, 2021. [Online]. Available: <http://arxiv.org/abs/2104.06084>

- [10] M. C. Coşkun and H. D. Pfister, "An information-theoretic perspective on successive cancellation list decoding and polar code design," *IEEE Trans. Inf. Theory*, submitted, 2021. [Online]. Available: <http://arxiv.org/abs/2103.16680>
- [11] I. Dumer, "Recursive decoding and its performance for low-rate Reed-Muller codes," *IEEE Trans. Inf. Theory*, vol. 50, no. 5, pp. 811–823, May 2004.
- [12] —, "Soft-decision decoding of Reed-Muller codes: a simplified algorithm," *IEEE Trans. Inf. Theory*, vol. 52, no. 3, pp. 954–963, Mar. 2006.
- [13] I. Dumer and K. Shabunov, "Soft-decision decoding of Reed-Muller codes: recursive lists," *IEEE Trans. Inf. Theory*, vol. 52, no. 3, pp. 1260–1266, Mar. 2006.
- [14] K. Niu and K. Chen, "CRC-aided decoding of polar codes," *IEEE Commun. Lett.*, vol. 16, no. 10, pp. 1668–1671, 2012.
- [15] V. Miloslavskaya and P. Trifonov, "Sequential decoding of polar codes," *IEEE Commun. Lett.*, vol. 18, no. 7, pp. 1127–1130, 2014.
- [16] P. Trifonov, "A score function for sequential decoding of polar codes," *IEEE Int. Symp. Inf. Theory (ISIT)*, pp. 1470–1474, 2018.
- [17] M.-O. Jeong and S.-N. Hong, "SC-Fano decoding of polar codes," *IEEE Access*, vol. 7, pp. 81 682–81 690, 2019.
- [18] B. Li, H. Shen, and D. Tse, "A RM-polar codes," *CoRR*, vol. abs/1407.5483, 2014. [Online]. Available: <http://arxiv.org/abs/1407.5483>
- [19] M. Mondelli, S. H. Hassani, and R. L. Urbanke, "From polar to Reed-Muller codes: A technique to improve the finite-length performance," *IEEE Trans. Commun.*, vol. 62, no. 9, pp. 3084–3091, Sep. 2014.
- [20] O. Afisiadis, A. Balatsoukas-Stimming, and A. Burg, "A low-complexity improved successive cancellation decoder for polar codes," in *Asilomar Conf. Signals, Syst., Comput.*, 2014, pp. 2116–2120.
- [21] L. Chandesaris, V. Savin, and D. Declercq, "Dynamic-SCFlip decoding of polar codes," *IEEE Trans. Commun.*, vol. 66, no. 6, pp. 2333–2345, 2018.
- [22] I. Tal and A. Vardy, "List decoding of polar codes," *IEEE Trans. Inf. Theory*, vol. 61, no. 5, pp. 2213–2226, 2015.
- [23] P. Trifonov and V. Miloslavskaya, "Polar subcodes," *IEEE J. Sel. Areas Commun.*, vol. 34, no. 2, pp. 254–266, Feb. 2016.
- [24] T. Wang, D. Qu, and T. Jiang, "Parity-check-concatenated polar codes," *IEEE Commun. Lett.*, vol. 20, no. 12, pp. 2342–2345, 2016.
- [25] M. Qin, J. Guo, A. Bhatia, A. Guillén i Fàbregas, and P. H. Siegel, "Polar code constructions based on LLR evolution," *IEEE Commun. Lett.*, vol. 21, no. 6, pp. 1221–1224, Jun. 2017.
- [26] S. A. Hashemi, N. Doan, M. Mondelli, and W. J. Gross, "Decoding Reed-Muller and polar codes by successive factor graph permutations," in *IEEE Int. Symp. Turbo Codes & Iterative Inf. Process.*, 2018, pp. 1–5.
- [27] M. Ye and E. Abbe, "Recursive projection-aggregation decoding of Reed-Muller codes," in *IEEE Int. Symp. Inf. Theory*, Jul. 2019, pp. 2064–2068.
- [28] K. Ivanov and R. Urbanke, "Permutation-based decoding of Reed-Muller codes in binary erasure channel," in *IEEE Int. Symp. Inf. Theory*, Jul. 2019, pp. 21–25.
- [29] P. Yuan, T. Prinz, G. Böcherer, O. İşcan, R. Böhnke, and W. Xu, "Polar code construction for list decoding," in *Proc. 11th Int. ITG Conf. on Syst., Commun. and Coding (SCC)*, Feb. 2019, pp. 125–130.
- [30] E. Arıkan, "From sequential decoding to channel polarization and back again," *CoRR*, vol. abs/1908.09594, 2019. [Online]. Available: <http://arxiv.org/abs/1908.09594>
- [31] M. C. Coşkun, J. Neu, and H. D. Pfister, "Successive cancellation inactivation decoding for modified Reed-Muller and eBCH codes," in *IEEE Int. Symp. Inf. Theory*, 2020, pp. 437–442.
- [32] B. Li, J. Gu, and H. Zhang, "Performance of CRC concatenated pre-transformed RM-polar codes," *CoRR*, vol. abs/2104.07486, 2021. [Online]. Available: <http://arxiv.org/abs/2104.07486>
- [33] B. Li, H. Zhang, and J. Gu, "On pre-transformed polar codes," *CoRR*, vol. abs/1912.06359, 2019. [Online]. Available: <http://arxiv.org/abs/1912.06359>
- [34] H. Yao, A. Fazeli, and A. Vardy, "List decoding of Arıkan's PAC codes," in *IEEE Int. Symp. Inf. Theory*, 2020, pp. 443–448.
- [35] M. Rowshan, A. Burg, and E. Viterbo, "Polarization-adjusted convolutional (PAC) codes: Sequential decoding vs list decoding," *IEEE Trans. Veh. Technol.*, vol. 70, no. 2, pp. 1434–1447, 2021.
- [36] M. C. Coşkun and H. D. Pfister, "Bounds on the list size of successive cancellation list decoding," in *Int. Conf. on Signal Process. and Commun. (SPCOM)*, 2020, pp. 1–5.
- [37] Y. Li, H. Zhang, R. Li, J. Wang, G. Yan, and Z. Ma, "On the weight spectrum of pre-transformed polar codes," *CoRR*, vol. abs/2102.12625, 2021. [Online]. Available: <http://arxiv.org/abs/2102.12625>
- [38] M. Rowshan and E. Viterbo, "How to modify polar codes for list decoding," in *Proc. IEEE Int. Symp. Inf. Theory*, Jul. 2019, pp. 1772–1776.
- [39] M. Kamenov, Y. Kamenova, O. Kurmaev, and A. Maevskiy, "Permutation decoding of polar codes," in *XVI Int. Symp. "Problems of Redundancy in Information and Control Systems"*, 2019, pp. 1–6.
- [40] V. Miloslavskaya and B. Vucetic, "Design of short polar codes for SCL decoding," *IEEE Trans. Commun.*, vol. 68, no. 11, pp. 6657–6668, 2020.
- [41] M. Geiselhart, A. Elkelesh, M. Ebada, S. Cammerer, and S. ten Brink, "Automorphism ensemble decoding of Reed-Muller codes," *CoRR*, vol. abs/2012.07635, 2020. [Online]. Available: <http://arxiv.org/abs/2012.07635>
- [42] —, "On the automorphism group of polar codes," *CoRR*, vol. abs/2101.09679, 2021. [Online]. Available: <http://arxiv.org/abs/2101.09679>
- [43] T. Tonnellier and W. J. Gross, "On systematic polarization-adjusted convolutional (PAC) codes," *IEEE Commun. Lett.*, pp. 1–1, 2021.
- [44] Y. Polyanskiy, V. Poor, and S. Verdù, "Channel coding rate in the finite blocklength regime," *IEEE Trans. Inf. Theory*, vol. 56, no. 5, pp. 2307–235, May 2010.
- [45] G. Forney, "Exponential error bounds for erasure, list, and decision feedback schemes," *IEEE Trans. Inf. Theory*, vol. 14, no. 2, pp. 206–220, 1968.
- [46] R. Fano, "A heuristic discussion of probabilistic decoding," *IEEE Trans. Inf. Theory*, vol. 9, no. 2, pp. 64–74, 1963.
- [47] B. Dorsch, "A decoding algorithm for binary block codes and J-ary output channels (corresp.)," *IEEE Trans. Inf. Theory*, vol. 20, no. 3, pp. 391–394, 1974.
- [48] M. Fossorier and S. Lin, "Soft-decision decoding of linear block codes based on ordered statistics," *IEEE Trans. Commun.*, vol. 41, no. 5, pp. 1379–1396, Sep. 1995.
- [49] Y. Wu and C. N. Hadjicostis, "Soft-decision decoding using ordered recodings on the most reliable basis," *IEEE Trans. Inf. Theory*, vol. 53, no. 2, pp. 829–836, 2007.
- [50] R. Mori and T. Tanaka, "Performance and construction of polar codes on symmetric binary-input memoryless channels," in *Proc. IEEE Int. Symp. on Inf. Theory*, Seoul, Jun. 2009, pp. 1496–1500.
- [51] A. Balatsoukas-Stimming, M. B. Parizi, and A. Burg, "LLR-based successive cancellation list decoding of polar codes," *IEEE Trans. Signal Process.*, vol. 63, no. 19, pp. 5165–5179, 2015.
- [52] I. Jacobs and E. Berlekamp, "A lower bound to the distribution of computation for sequential decoding," *IEEE Trans. Inf. Theory*, vol. 13, no. 2, pp. 167–174, 1967.
- [53] G. He, J. Belfiore, I. Land, G. Yang, X. Liu, Y. Chen, R. Li, J. Wang, Y. Ge, R. Zhang, and W. Tong, "Beta-expansion: A theoretical framework for fast and recursive construction of polar codes," *IEEE Global Telecommun. Conf. (GLOBECOM)*, pp. 1–6, 2017.
- [54] E. Hof, I. Sason, and S. Shamai, "Performance bounds for erasure, list, and decision feedback schemes with linear block codes," *IEEE Trans. Inf. Theory*, vol. 56, no. 8, pp. 3754–3778, 2010.